HHS Public Access

Author manuscript

Eur J Nucl Med Mol Imaging. Author manuscript; available in PMC 2016 January 21.

Published in final edited form as:

Eur J Nucl Med Mol Imaging. 2010 July ; 37(7): 1300–1308. doi:10.1007/s00259-010-1396-2.

FDG positron emission tomography/computed tomography studies of Wilms' tumor

A. K. M. Moinul Hossain,
Nuclear Imaging Division, Department of Radiological Sciences, MS #220, St. Jude Children's Research Hospital, 262 Danny Thomas Place, Memphis, TN 38105-3678, USA

Barry L. Shulkin,
Nuclear Imaging Division, Department of Radiological Sciences, MS #220, St. Jude Children's Research Hospital, 262 Danny Thomas Place, Memphis, TN 38105-3678, USA

Michael J. Gelfand,
Department of Radiology, Cincinnati Children's Hospital Medical Center, Cincinnati, OH, USA

Humayun Bashir,
Medical Imaging, King Abdul Aziz Medical City, Riyadh, Saudi Arabia

Najat C. Daw,
Department of Oncology, St. Jude Children's Research Hospital, Memphis, TN, USA

Susan E. Sharp,
Department of Radiology, Cincinnati Children's Hospital Medical Center, Cincinnati, OH, USA

Helen R. Nadel, and
Division of Nuclear Medicine, Department of Radiology, British Columbia Children's Hospital, Vancouver, BC, Canada

Jeffrey S. Dome
Division of Oncology, Children's National Medical Center, Washington, DC, USA

Barry L. Shulkin: barry.shulkin@stjude.org

Abstract

Purpose—The purpose of this analysis was to evaluate the utility of FDG PET/CT scanning in patients with Wilms' tumors.

Methods—A total of 58 scans were performed in 27 patients (14 male, 13 female; ages: 1.9–23 years, median: 7 years) with proven Wilms' tumor. Twenty-six patients (56 scans) were studied at the time of suspected relapse, progressive disease, persistent disease, or for monitoring of therapy.

Results—In the 27 patients with Wilms' tumor, 34 scans showed areas of abnormal uptake consistent with metabolically active tumors. Of the patients, 8 (24 scans) had pulmonary metastases larger than 10 mm in diameter, 10 (12 scans) had hepatic metastases, 11 (11 scans) had regional nodal involvement, 3 (3 scans) had bone metastases, 1 (1 scan) had chest wall

Correspondence to: Barry L. Shulkin, barry.shulkin@stjude.org.

Presented in part at the 55th Annual Conference of the Society of Nuclear Medicine, New Orleans, LA.

involvement, 2 (2 scans) had pancreatic metastasis, and 5 (5 scans) had abdominal and pelvic soft tissue involvement. Two of eight patients with lung metastases had variable uptakes. Lung lesions 10 mm or smaller were not consistently visualized on PET scans. One patient with a liver metastasis showed no uptake on PETscan after treatment (size decreased from 45 to 15 mm).

Conclusion—Most Wilms' tumors concentrate FDG. However, small pulmonary metastases may be better visualized with CT. FDG PET/CT appears useful for defining the extent of involvement and assessing the response to treatment.

Keywords

FDG PET/CT; Wilms' tumor; Metabolism; FDG; Pediatrics

Introduction

Wilms' tumor, the most common primary malignant renal tumor of childhood, accounts for 6% of all pediatric cancer in the USA. Approximately 8 cases are found annually per million children under the age of 15 years [1]. The mean age of patients with Wilms' tumor at diagnosis is approximately 3.5 years, and 75% are younger than 5 years [2]. The median age is 39 months for those with unilateral disease and 27 months for those with bilateral disease [3]. Treatment of Wilms' tumor is largely based on the histopathologic classification of the tumor (favorable versus anaplastic histology) and on surgical stage. The long-standing approach used by the National Wilms' Tumor Study Group for a unilateral tumor is a nephrectomy at the time of diagnosis, followed by chemotherapy; the use of radiation therapy depends on the extent of disease within the abdomen and presence of metastatic disease [2]. Disease staging is based on surgical findings and imaging studies that determine presence of metastasis. Disease evaluation prior to nephrectomy includes computed tomography (CT) scans, which reveal the size and location of the primary tumor, lymph node enlargement, and distant metastases. However, findings on CT do not predict tumor involvement by histology, thus creating the need for imaging modalities that can provide better predictive staging assessment.

Wilms' tumors are metabolically active. We have previously shown [4] that they accumulate ^{18}F-fluorodeoxyglucose (FDG) and can thus be visualized using positron emission tomography (PET) [4, 5]. PET imaging using FDG has potential advantages over conventional imaging in pediatric tumor staging, grading, and assessing tumor response to preoperative chemotherapy, and disease surveillance in many tumors in the pediatric population.

The fusion of PET and CT has been used successfully in the diagnosis, staging, monitoring of response to therapy, and surveillance of various malignancies in adult and selected pediatric patients [5]. PET/CT is useful for identifying the most metabolically active portion of a lesion for biopsy, staging, monitoring response (restaging) to chemotherapy, and disease surveillance. Interpretations based on fused PET/CT data proved significantly more accurate than those based on CT images alone, PET data alone, or side-by-side PET and CT when assessing the overall tumor, node, metastasis system stages of various malignant diseases [6].

To evaluate the role of FDG PET/CT in the management of patients with Wilms' tumors, we conducted a retrospective analysis of our experience with FDG PET/ CT since this technique became available at St. Jude Children's Research Hospital (SJCRH) (September 2002), Cincinnati Children's Hospital Medical Center (February 2006), and Vancouver Children's Hospital (July 2005).

Materials and methods

This study was approved by the Institutional Review Boards of the three participating institutions. The study consisted of a review of patient imaging studies and medical records for diagnosis, treatment, and demographic data.

Patients

A total of 58 scans were performed in 27 patients (14 male, 13 female; ages: 1.9–23 years, median: 7 years) with proven Wilms' tumor. Among them, 21 patients were examined for recurrence, 5 for treatment assessment on a phase II study of topotecan [7], 2 for baseline study after surgery and before other treatment, and 1 for monitoring radiofrequency ablation. Some patients were examined for a combination of these reasons.

At the time of diagnosis, there were two patients with stage 1, six patients with stage 2, seven patients with stage 3, nine patients with stage 4, and three patients with stage 5 disease. Eighteen had favorable histology, four unfavorable, and five not specified.

PET/CT method

After a 4-h or overnight fast, the patients were given intravenous injections of ~0.15 mCi/kg ^{18}F-FDG (maximum 12 mCi). Approximately 1 h later, after the patient voided, image acquisition began with a CT scan for attenuation correction and lesion localization. In 17 patients (3–6, 14–19, 22–27), the CT was performed using 120 kVp and 15–100 mAs without iodinated contrast; in 8 patients (1, 2, 7, 9–11, 20, 21), CT parameters were 120 kVp and 30–35 mAs without iodinated contrast. Two patients (12, 13) received intravenous contrast; the CT acquisition parameters were 80–100 kVp and 40–80 mAs. The CT was followed by emission imaging using a GE Discovery LS PET/CT scanner (SJCRH), GE Discovery STE (Cincinnati Children's Hospital), and Siemens Biograph (Vancouver Children's Hospital). Emission imaging times per bed position were 5, 4, and 3 min, respectively.

Of the 27 patients, 26 were imaged with arms at the side and 1 with arms raised. In all patients, the minimum area scanned was the base of the neck through the pelvis, although most included the upper extremities and proximal lower extremities. Both PET and CT images were reviewed and interpreted, both qualitatively and semiquantitatively, by two nuclear medicine physicians concurrently and one nuclear medicine physician at Vancouver Children's Hospital (two patients, three scans). Foci of uptake not explained by the expected biodistribution of FDG, physiological variants, or other pathological causes were considered abnormal.

Results

Twenty-seven patients with Wilms' tumor underwent disease evaluation with PET/CT scans. Nine patients had more than one scan (range: 2–9 scans); a total of 58 scans were obtained. Of 27 patients (28 scans), 18 had areas of abnormally increased FDG uptake on one or more PET/CT scans. Areas of increased uptake were detected in the lung, pulmonary hilum, bone, liver, retroperitoneum, pelvis, neck, chest wall, and pancreas (Figs. 1, 2, 3, 4, and 5).

All lesions detected by PET scan were also visualized by CT scan. However, 11 CT scans in 10 patients detected lesions that were not visualized by PET scan. Most of these lesions were lung nodules that were less than 10 mm in diameter. Additionally, a 24-mm liver lesion, a 10-mm liver lesion, an 18-mm mesenteric lymph node, and a 27-mm sclerotic bone lesion after treatment were detected on CT scan but not PET scan.

In all 27 patients, areas of abnormal uptake consistent with metabolically active tumors were seen in 34 scans (Table 1). Eight patients (24 scans) had lung metastases larger than 10 mm. Eleven patients (11 scans) were positive for regional nodal involvement. Ten patients (12 scans) had liver metastases, one of which decreased in diameter from 45 to 15 mm after treatment. Three patients (three scans) had bone metastases, one patient (one scan) had chest wall involvement, and two patients (two scans) had pancreatic metastasis. Five patients (five scans) had abdominal and pelvic soft tissue involvement. Of eight patients with lung metastases, two had variable uptake; lung lesions 10 mm or less in diameter were most commonly not visualized on the PET scan.

There were three patients with CT masses 10 mm or larger whose post-therapy FDG PET/CT studies showed residual anatomic abnormalities without FDG uptake. In patient 4, a 11-mm lung metastasis showed no uptake following therapy, consistent with successful radiofrequency ablation. In patient 27, follow-up MRI showed low signal on T1 and T2 sequences suggesting hemosiderosis following therapy.

Discussion

This study represents a 6-year experience from three pediatric institutions of the use of FDG PET/CT in the evaluation of patients with Wilms' tumors. Although our study contains selection bias due to selection of patients with metastatic disease who had failed therapy, it confirms previous observations that Wilms' tumor is FDG-avid and indicates that FDG PET/CT may be a useful adjunct to conventional imaging studies. A growing body of data supports a role for FDG PET/CT scans in the management of pediatric cancer. The most established use of PET scans in children is for staging and monitoring of Hodgkin's disease (HD) and non-Hodgkin's lymphoma (NHL) [8, 9].

Miller et al. [10] found greater accuracy of staging with PET/CT than conventional imaging in a series of patients with lymphoma; there was a change in staging at the time of diagnosis in about one third of pediatric patients with HD and NHL. The current Children's Oncology Group research treatment protocols for children and adolescents with newly diagnosed intermediate-risk HD and advanced-stage anaplastic large-cell NHL require PET or gallium

imaging before therapy, followed by repeat imaging to assess treatment response after chemotherapy.

For Wilms' tumor, the use of PET/CT scans may be considered in several clinical settings: the diagnostic workup, the evaluation of recurrent disease, and the monitoring of chemotherapy response.

The diagnostic workup

The standard radiologic evaluation of newly diagnosed Wilms' tumor includes a CT or MRI scan of the abdomen and pelvis to visualize the primary tumor, the contralateral kidney, lymph nodes, and intra-abdominal or pelvic tumor deposits. A Doppler ultrasound is recommended as a complementary test to evaluate tumor thrombus in the renal vein and inferior vena cava. Misch et al. [11] performed FDG PET/CT scans on nine patients with newly diagnosed Wilms' tumor and found perfect concordance between the PET/CT and conventional imaging studies. None of the patients in that series had metastatic disease. Chest X-rays have historically been used to detect lung metastases, but CT scans are more sensitive in detecting small nodules or effusions [12–15]. A pitfall of CT scans is that they are not specific for tumor. On the fifth National Wilms' Tumor Study, lung nodules detected on CT scan but not chest X-ray were confirmed to be tumor in only 74% of patients who underwent biopsy [16]. PET scanning has the potential to distinguish tumor-containing lung nodules from benign lesions. However, our data indicate that FDG PET is not sensitive for lung nodules less than 10 mm in diameter. Although our data were obtained in patients who had been treated, we believe the findings are also applicable at diagnosis, in part due to the intrinsic limited resolution of PET imaging. It is therefore unlikely that FDG PET will solve the diagnostic dilemma of small lung nodules in patients with Wilms' tumor. Unlike the study of Misch et al., in this study, only one of the patients was studied prior to therapy.

Nonetheless, because most Wilms' tumors are unilateral and usually cured by surgery alone, we do not expect that FDG PET/CT scans will serve an important role in the staging of most patients with Wilms' tumor [11].

Evaluation of recurrent disease

Wilms' tumor recurs predominantly in the lung, tumor bed, regional lymph nodes, distal urinary tract, and liver, although it may recur elsewhere in the body. In our series, FDG PET scans detected metastases in bone, extra-abdominal lymph nodes, chest wall, and pancreas. These lesions were also detectable by conventional CT scan, but it is possible that PET drew attention to these unconventional metastatic sites that otherwise might have gone unnoticed. Misch et al. [11] reported a patient with recurrent Wilms' tumor in whom FDG PET revealed retroperitoneal lymph node involvement and peritoneal tumor deposits that were not detected on conventional imaging studies [11]. PET should therefore be considered in the restaging evaluation of patients with recurrent disease.

Monitoring of chemotherapy response

Functional imaging studies, such as FDG PET scans, can be used to monitor the metabolic response to therapy, which may be discordant from the anatomic response. Some Wilms'

tumors, including stromal- and epithelial-predominant subtypes, differentiate in response to therapy and do not contract anatomically. As described above, there were three patients with CT masses 10 mm or larger whose post-therapy FDG PET/CT studies showed residual anatomic abnormalities without FDG uptake. Patient 4 in our series had slow-growing epithelial-predominant lung metastases that showed about 50% decrease in size in response to chemotherapy and resolution of FDG uptake. The patient ultimately had tumor progression and was treated with multiple courses of radiofrequency ablation, with a concomitant decrease in FDG uptake. The PET scans helped guide which lung lesions to target. In patient 27, whose initial FDG PET/CT showed uptake in a large hepatic lesion, there was no uptake in the residual 24-mm mass following treatment. Follow-up MRI showed signal abnormalities consistent with hemosiderosis following therapy. In patient 20, a right lower quadrant 18-mm lymph node remained stable in size on follow-up CT 6 months after the FDG PET/CT scan. It was excised 1 month later, showing follicular hyperplasia with no evidence of tumor. These cases illustrate that PET can be useful to monitor the therapeutic response of Wilms' tumor and can be particularly valuable for tumors that are not amenable to surgical resection.

In our series, most small lung lesions without FDG uptake were considered malignant clinically at the time of the study, but the clinical course can yield additional information. In patient 3, the 4-mm nodule was unchanged 14 months after the PET/CT scan and considered to be granulomatous disease based on the stability; 5 years later, the chest radiograph is normal. Thus, the lesion is most likely benign. In patient 22, the nodule enlarged and two additional lung nodules appeared, consistent with progressive disease. The lung nodules resolved after further chemotherapy, but the patient suffered relapse and died 16 months after the FDG PET/CT scan. In patient 17, the small lesions seen on CT that were not FDG-avid were considered pulmonary metastases because the patient developed brain metastases and died from progressive disease.

There was no clear difference in FDG uptake between patients with favorable and unfavorable histologies. Of four patients with unfavorable histologies, two had no uptake and one had uptake that could not be quantified; thus only one patient with unfavorable histology had quantifiable uptake. We cannot exclude differences in uptake between histologies due to the limited number of evaluable patients with unfavorable histology. Since only one patient was studied at diagnosis, differences in uptake at the time of presentation also cannot be determined. However, in the study of Misch et al., at the time of initial staging, there was no definite difference in uptake in two patients with anaplastic histology compared with nine patients who had intermediate-risk histology [11].

Conclusion

We have shown that Wilms' tumor is metabolically active and concentrates FDG. However, small pulmonary metastases (<10 mm) are better visualized by CT. Further studies may be useful to assess the utility of FDG PET/CT scans for the workup of recurrent Wilms' tumor and measuring response to chemotherapy in patients with unresectable disease.

Acknowledgments

Supported in part by US Public Health Service Center Support Grant CA 21765 and by the American Lebanese Syrian Associated Charities (ALSAC).

We thank David Galloway for editorial review, Sandra Gaither for her assistance in preparing the manuscript, the British Nuclear Medicine Society Travelling Fellowship (HB), and special thanks to Syeda Hasnaher Hossain for lifelong inspiration.

References

1. Ries, LAG.; Eisner, MP.; Kosary, CL.; Hankey, BF.; Miller, BA.; Clegg, L., et al., editors. SEER Cancer Statistics Review, 1975–2000. Bethesda, MD: National Cancer Institute; 2003.
2. Dome, JS.; Perlman, EJ.; Richey, ML., et al. Renal tumors. In: Pizzo, PA.; Poplack, DG., editors. Principles and practice of pediatric oncology. Philadelphia: Lippincott Williams & Wilkins; 2006. p. 905-32.
3. Breslow N, Olshan A, Beckwith JB, Green DM. Epidemiology of Wilms tumor. Med Pediatr Oncol. 1993; 21(3):172–81. [PubMed: 7680412]
4. Shulkin BL, Chang E, Strouse PJ, Bloom DA, Hutchinson RJ. PET FDG studies of Wilms tumors. J Pediatr Hematol Oncol. 1997; 19(4):334–8. [PubMed: 9256833]
5. Federman N, Feig SA. PET/CT in evaluating pediatric malignancies: a clinician's perspective. J Nucl Med. 2007; 48(12):1920–2. [PubMed: 18056331]
6. Antoch G, Saoudi N, Kuehl H, Dahmen G, Mueller SP, Beyer T, et al. Accuracy of whole-body dual-modality fluorine-18-2-fluoro-2-deoxy-D-glucose positron emission tomography and computed tomography (FDG-PET/CT) for tumor staging in solid tumors: comparison with CT and PET. J Clin Oncol. 2004; 22(21):4357–68. [PubMed: 15514377]
7. Metzger ML, Stewart CF, Freeman BB 3rd, Billups CA, Hoffer FA, Wu J, et al. Topotecan is active against Wilms' tumor: results of a multi-institutional phase II study. J Clin Oncol. 2007; 25(21): 3130–6. [PubMed: 17634492]
8. Kostakoglu L, Goldsmith SJ. Fluorine-18 fluorodeoxyglucose positron emission tomography in the staging and follow-up of lymphoma: is it time to shift gears? Eur J Nucl Med. 2000; 27(10):1564–78. [PubMed: 11083548]
9. Rehm PK. Radionuclide evaluation of patients with lymphoma. Radiol Clin North Am. 2001; 39(5): 957–78. [PubMed: 11587064]
10. Miller E, Metser U, Avrahami G, Dvir R, Valdman D, Sira LB, et al. Role of 18F-FDG PET/CT in staging and follow-up of lymphoma in pediatric and young adult patients. J Comput Assist Tomogr. 2006; 30(4):689–94. [PubMed: 16845304]
11. Misch D, Steffen IG, Schönberger S, Voelker T, Furth C, Stöver B, et al. Use of positron emission tomography for staging, preoperative response assessment and posttherapeutic evaluation in children with Wilms tumour. Eur J Nucl Med Mol Imaging. 2008; 35(9):1642–50. [PubMed: 18509634]
12. Wilimas JA, Douglass EC, Magill HL, Fitch S, Hustu HO. Significance of pulmonary computed tomography at diagnosis in Wilms' tumor. J Clin Oncol. 1988; 6(7):1144–6. [PubMed: 2839631]
13. Wilimas JA, Kaste SC, Kauffman WM, Winer-Muram H, Morris R, Luo X, et al. Use of chest computed tomography in the staging of pediatric Wilms' tumor: interobserver variability and prognostic significance. J Clin Oncol. 1997; 15(7):2631–5. [PubMed: 9215834]
14. Green DM, Fernbach DJ, Norkool P, Kollia G, D'Angio GJ. The treatment of Wilms' tumor patients with pulmonary metastases detected only with computed tomography: a report from the National Wilms' Tumor Study. J Clin Oncol. 1991; 9(10):1776–81. [PubMed: 1655987]
15. Meisel JA, Guthrie KA, Breslow NE, Donaldson SS, Green DM. Significance and management of computed tomography detected pulmonary nodules: a report from the National Wilms Tumor Study Group. Int J Radiat Oncol Biol Phys. 1999; 44(3):579–85. [PubMed: 10348287]
16. Ehrlich PF, Hamilton TE, Grundy P, Ritchey M, Haase G, Shamberger RC, et al. The value of surgery in directing therapy for patients with Wilms' tumor with pulmonary disease. A report from

the National Wilms' Tumor Study Group (National Wilms' Tumor Study 5). J Pediatr Surg. 2006; 41(1):162–7. [PubMed: 16410127]

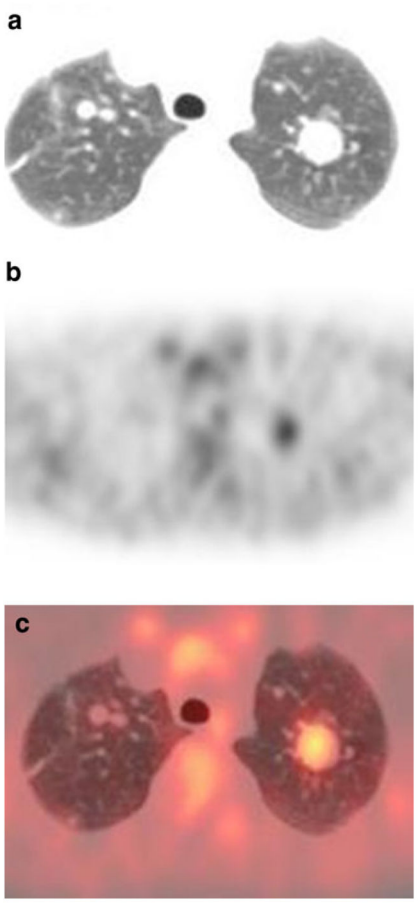

Fig. 1.

Patient 4: 9-year-old girl with bilateral lung metastases. **a** Transverse CT image of the lungs (lung window). **b** FDG PET at same level as **a. c** Fusion image of **a** and **b**. The largest lesion in the left upper lobe shows uptake higher than background lung. Smaller pulmonary lesions in the right upper lobe are not evident on the PET scan

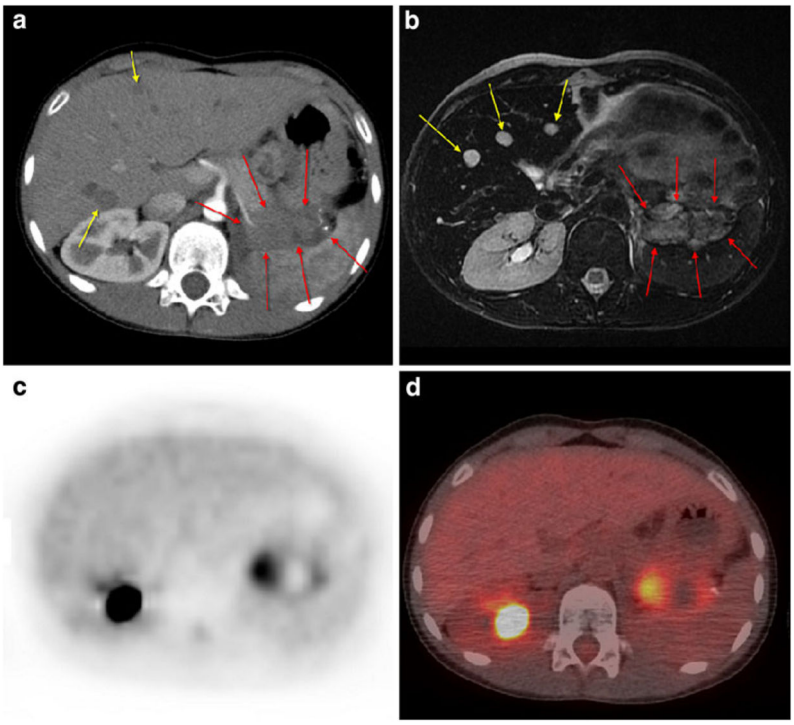

Fig. 2.

Patient 7: 10-year-old girl with left-sided recurrent Wilms' tumor showing two liver metastases (*yellow arrows*) on contrast-enhanced CT (**a**) and three foci on MRI (**b**) not detectable on PET scan (**c**) or on PET/CT fusion image (**d** without intravenous contrast). The lesion in the pancreatic tail area (*red arrows* on **a** and **b**) is evident in all images

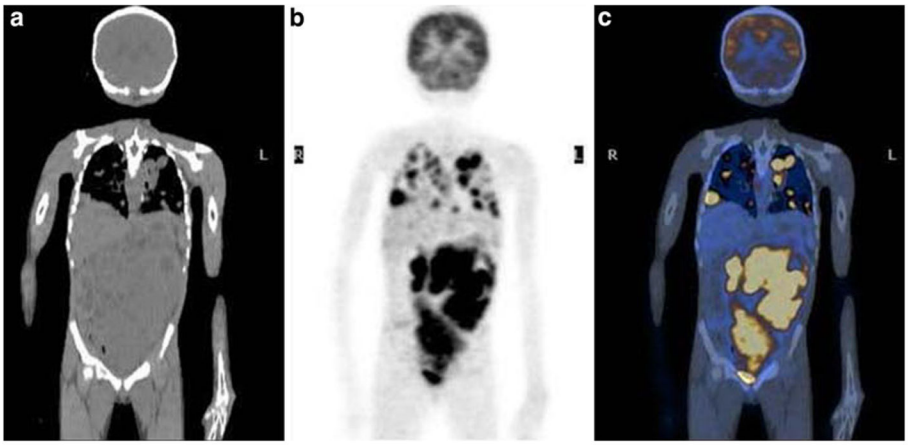

Fig. 3.

Patient 16: 7-year-old girl with newly diagnosed right-sided Wilms' tumor showing extensive metastatic disease in the chest, abdomen, and pelvis. **a** Noncontrast coronal CT image of the abdomen. **b** FDG PET at same level as **a. c** Fusion image of **a** and **b**

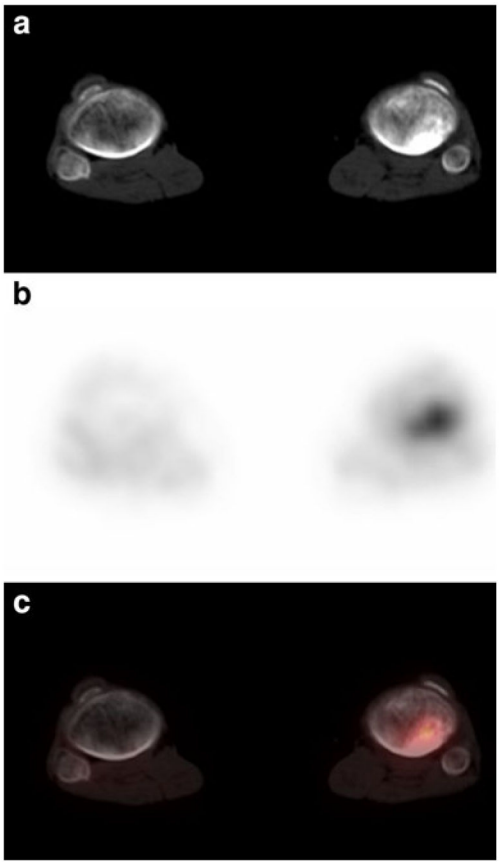

Fig. 4.

Patient 17: 11-year-old girl with recurrent Wilms' tumor showing focal uptake and sclerotic process in the left proximal tibia; consistent with bony metastatic disease. **a** Noncontrast transverse CT image of the distal lower extremities (bone window). **b** FDG PET at same level as **a. c** Fusion image of **a** and **b**

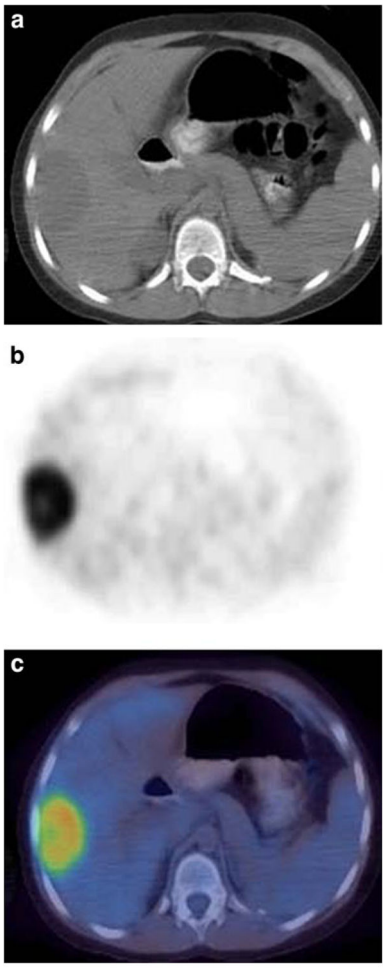

Fig. 5.

Patient 27: 8-year-old girl with recurrent Wilms' tumor showing focal uptake in the liver consistent with metastatic disease. **a** Noncontrast transverse CT image of the abdomen. **b** FDG PET at same level as **a. c** Fusion image of **a** and **b**

Table 1

Demographic, diagnosis, and treatment data for 27 patients with Wilms' tumor

Pat. No.	Age (years)	Sex	Tumor histology & site	Stage at dx	Patient scan # & ind	PET finding	SUV_{max}	CT finding
1	3	M	FAVORAB, right	1	1 Recur (rule out)	NED	NA	18 mm focus in right lower abdomen (possible mesenteric lymph node)
2	2	M	FAVORAB, right	1	1 Recur (rule out)	NED	NA	6 mm portocaval nodes
3	5	F	UN-DA, right	2	1 Recur	NED	NA	Left lung focus (<4 mm)
4	9	F	FAVORAB, right	2	1 Recur	3 foci in lung	3.1	At least 7 foci measurable maximum size 20 mm
					2 Recur	Marked decreased in lung uptake	2.2	Maximum size 13 mm
					3 Recur	Minimal uptake of lung foci	1.3	Size unchanged 13 mm
					4 Recur	No change	1.3	Size unchanged 13 mm
					5 Recur	No change	No uptake	Size decreased 11 mm
					6 Recur	PD after RFA: increased size of 2 lung foci	2.7	Maximum size 32 mm
					7 Recur	Right upper lung focus (post-RFA)	1.1	Maximum size 5 mm
					8 Recur	No interval progression of disease	1.4	Maximum size 16 mm
					9 RFA response	Variable uptakes of lung foci	5.9	Maximum size 25 mm
5	4	F	NOS, left	2	1 Recur	NED	NA	NED
6	4	M	FAVORAB, left	2	1 Recur	Left lower lung focus	1.8	10 mm
7	10	F	NS, left	2	1 Recur	NED	NA	Stable liver foci
					2 Recur	NED	NA	Increased size of liver foci, later became stable
					3 Recur	Left liver foci	4.9	16 mm and 12 mm liver foci
					4 Recur	NED	NA	10 mm max. liver focus
					5 Recur	NED	NA	NED
					6 Recur	NED	NA	No study
					7 Recur	NED	NA	No study
					8 Recur	NED	NA	No study
					9 Recur	2 new foci in liver and pancreas	Liver 4 and pancreas 7.6	46 mm focus in pancreatic tail; 9 mm liver foci
8	23	M	FAVORAB, right	3	1 Recur	Right liver focus	9.1	98 mm

Eur J Nucl Med Mol Imaging. Author manuscript; available in PMC 2016 January 21.

Pat. No.	Age (years)	Sex	Tumor histology & site	Stage at dx	Patient scan # & ind	PET finding	SUV_{max}	CT finding
9	7	M	FAVORAB, left	3	1 Recur	Right upper mediastinal focus	4.3	33 mm
10	9	M	FAVORAB, left	3	1 Recur (prior)	NED	NA	NED
					2 Recur (prior)	NED	NA	NED
					3 Recur (prior)	NED	NA	NED
					4 Recur (prior)	NED	NA	NED
					5 Recur (prior)	NED	NA	NED
					6 Recur (prior)	NED	NA	NED
					7 Recur (prior)	NED	NA	NED
						Mediastinal focus	Partial dose extravasation	10 mm
						Right hilar focus		11 mm
11	2	F	NS, right	3	1 Refractory	Multiple foci in abdomen, liver and supraclavicular area	Liver 8.3; abdomen 7.2 and supraclavicular 5.2	44 mm liver focus; 55 mm abdominal focus and 25 mm supraclavicular focus
12	7	M	FAVORAB, left	3	1 Recur	Right para-aortic and L2 vertebral body	3.9	27 mm soft tissue mass at L2 level and adjacent sclerotic lesion at L2
						Post-midthoracic paraspinal mass	3.2	25 mm
					2 Resp	NED		Sclerosis at L2
13	6	F	ANAPLAS, right	3	1 Recur	Multiple soft tissue foci including dome liver, tip of the spleen, right renal bed, para-aortic, mesenteric and pelvic	Unavailable	Not recorded
14	4	F	FAVORAB, extrarenal	3	1 End Rx	Supra bladder cystic focus (residual tumor)	Could not be assessed on outside study	
15	3	M	FAVORAB, right	4	1 Resp	Multiple right lung foci	2.2	12 mm (max. size)
						Left lobe liver focus	3.4	13 mm
					2 Resp	Lung foci almost resolved	NA	Very small lung focus (<2 mm)
						Liver focus resolved	NA	Liver focus resolved
					3 Recur	NED	NA	
					4 Recur	NED	NA	
					5 Recur	Right lung(new focus)	1.7	10 mm
16	7	F	FAVORAB, left	4	1 Base	Lung: multiple foci	5.1–8.6	Largest 30 mm
						Multiple liver foci	6.3–9.0	10–30 mm
						Left renal focus	8.1	95 mm

Pat. No.	Age (years)	Sex	Tumor histology & site	Stage at dx	Patient scan # & ind	PET finding	SUV_{max}	CT finding
					2 Resp	NED	NA	Very small lung foci
17	11	F	FAVORAB, right	4	1 Recur	Bilateral small lung foci	NA	Small lung foci <10 mm
						Para-aortic focus	7.5	15 mm
						Liver 2 foci	5.6	10 mm, 12 mm
						Retroperitoneal 2 foci	8.9	13 mm, 48 mm
						Pancreatic foci	8.6	35 mm
						Left tibial focus	5.9	30 mm
18	16	M	FAVORAB, left	4	1 Recur	Right hilar focus	2.7	15 mm
						Right lung focus	14.5	100 mm
						Right liver focus	13.5	90 mm
						Left liver focus	11.5	40 mm
					2 Recur	Right hilar focus	3.5	30 mm
						Right lung focus	10.1	110 mm
						Right lobe liver focus	11.1	72 mm
						Left lobe liver focus	9.6	53 mm
19	13	M	ANAPLAS, right	4	1 Base (after surgery)	Retroperitoneal focus	6.4	15 mm
						No pulmonary abnormalities		Bilateral lung foci <5 mm
20	9	F	NS, right & site	4	1 Recur (prior)	NED	NA	Negative
21	12	F	FAVORAB, left 7 mm lung focus	4	1	(persistence)	NED	NA
			8 mm lung focus		2	(persistence)	NED	NA
22	4	F	FAVORAB, left	4	1 Recur	4 foci in right lung	Not accurate due to residual activity in injection line	4 foci (size: 16–20 mm)
						NED	NA	RML focus (<5 mm)
23	5	M	FAVORAB, left	4	1 Recur	Right lung focus	Not valid due to partial dose extravasation	20 mm
						Mediastinal focus		10 mm
						Right hilar focus		11 mm
24	12	F	FAVORAB, left	4	1 Resp	Active left lower lung with pleural focus consistent with metastatic disease	9.2	43 mm
25	2	M	UN-DA, bilateral	5	1 Recur	NED	NA	CT-guided needle biopsy at T11 level: negative for bone metastasis

Pat. No.	Age (years)	Sex	Tumor histology & site	Stage at dx	Patient scan # & ind	PET finding	SUV_{max}	CT finding
26	4	M	NOS, bilateral	5	1 Recur	NED	NA	NED
27	8	F	FAVORAB, bilateral	5	1 Resp	Liver focus	10.9	48 mm
						Right neck focus	2.7	14 mm
						Left neck focus	2.4	7 mm
						Left Internal mammary focus	2.4	11 mm
					2 Resp	NED	NA	24 mm Liver focus

Pat. patient, *dx* diagnosis, *ind* indication, *PET* positron emission tomography, *SUV* standardized uptake value, *CT* computed tomography, *Recur* recurrent disease, *RFA* radiofrequency ablation, *End RX* end-of-treatment assessment, *Resp* treatment response assessment, *Base* baseline (pretreatment) assessment, *NED* no evidence of disease, *RML* right middle lobe, *PD* progressive disease, *NOS* not otherwise specified, *UN-DA* unfavorable histology diffuse anaplasia, *FAVORAB* favorable histology, *ANAPLAS* anaplastic histology, *NS* not stated, *NA* not applicable

Eur J Nucl Med Mol Imaging. Author manuscript; available in PMC 2016 January 21.